Molecular Crystals and Liquid Crystals Science and Technology. Section A. Molecular Crystals and Liquid Crystals

Publication details, including instructions for authors and subscription information:
http://www.tandfonline.com/loi/gmcl19

NEW CLASSIFICATION OF CHEVRONS IN ELECTROCONVECTION IN HOMEOTROPICALLY-ALIGNED NEMATICS

Jong-Hoon Huh [a b], Yoshiki Hidaka [a] & Shoichi Kai [a]

[a] Department of Applied Physics, Faculty of Engineering, Kyushu University, Fukuoka, 812-8581, Japan

[b] Department of Mechanical System Engineering, Faculty of Computer Science and Systems Engineering, Kyushu Institute of Technology, Iizuka-Shi, Fukuoka, 820-8502, Japan

Version of record first published: 24 Sep 2006

Mol. Cryst. and Liq. Cryst., 2001, Vol. 366, pp. 833-840
Reprints available directly from the publisher
Photocopying permitted by license only

New Classification of Chevrons in Electroconvection in Homeotropically-Aligned Nematics

JONG-HOON HUH*, YOSHIKI HIDAKA and SHOICHI KAI

Department of Applied Physics, Faculty of Engineering, Kyushu University, Fukuoka 812-8581, Japan

Two types of chevrons have been found in the conduction regime, as well as the conventional chevrons in the dielectric regime in homeotropically-aligned nematics. These two are named the defect-mediated chevron (DMC) and the defect-free chevron (DFC) by their structure changes. Two different bifurcation sequences are found with increasing the applied voltage, such as *Fréedericksz* transition → normal rolls → abnormal rolls → defect chaos → DMC for low frequencies and *Fréedericksz* transition → prewavy pattern → DFC for high frequencies. Moreover, the double periodicity of the chevrons (i.e., the short wavelength λ_1 of the striated rolls and the long wavelength λ_2 of the chevron bands) shows quite specific frequency dependence.

Keywords: electroconvection; chevrons; homeotropic alignment

INTRODUCTION

When one applies an alternating electric field across a thin nematic slab, one observes an electroconvection (EC) in a polarizing microscope [1-2]. EC provides a rich variety of pattern-formation phenomena in a dissipative system, and then it has been intensively studied for last three decades (see, e.g., Ref. [3-5]). The basic mechanism of electrohydrodynamic instability for EC is well understood in terms of the *Carr-Helfrich* effect [1-2]. The detail of EC patterns depends on the frequency f of the applied electric field $E(f)=E_0 cos(2\pi f t)$. At low frequencies, the charge relaxation time τ_c is much shorter than the period f^{-1} of the low-frequency

* Present address: Department of Mechanical System Engineering, Faculty of Computer Science and Systems Engineering, Kyushu Institute of Technology, Iizuka-Shi, Fukuoka 820–8502, Japan

electric field $E(f)$ ($\tau_\sigma f \ll 1$), while the director relaxation time τ_d is much larger than f^{-1} ($\tau_d f \gg 1$). Here the relaxation times are expressed by

$$\tau_\sigma = \frac{\varepsilon_0 \varepsilon_\perp}{\sigma_\perp} \quad , \quad \tau_d = \frac{\gamma_1 d^2}{\pi^2 K_{11}} \quad , \tag{1}$$

where $\varepsilon_{0,\perp}$, $\sigma_\perp$, γ_1, d, and K_{11} correspond to dielectric constants, electric conductivity, dynamic viscosity, sample thickness, and elastic constant, respectively [1, 4]. In this so-called conduction regime, therefore, since the director cannot follow the external field $E(f)$, the stationary convection occurs.

In the dielectric regime ($f > f_c$) above a certain cut-off frequency $f_c = O(\tau_\sigma^{-1})$, on the other hand, τ_σ becomes larger than f^{-1} ($\tau_\sigma f \gg 1$) and charges cannot accumulate. The director oscillates in phase with the alternating field $E(f)$, while the charge distribution is stationary [1]. In this dielectric regime, in general, there appear chevron patterns consisting of alternating stripes of zig and zag rolls with a very small wavelength ($\ll d$). Their width of the stripes (λ_2) is much larger than that of the rolls (λ_1).

Until now, almost the studies for chevrons have been performed in the planar geometry, whereas only a few studies have been done in the homeotropic case [6-7]. Moreover, almost the studies for chevrons in the both planar and homeotropic geometries were focused on the conventional chevrons in the dielectric regime. The previous studies mainly devoted to the dependence of the threshold and the wavelength (λ_1) of striated zig and zag rolls in chevrons with respect to the applied frequency f, thickness d, electric conductivities $\sigma_{//,\perp}$, dielectric constants $\varepsilon_{//,\perp}$, or the strength of stabilizing magnetic field H [6]. Very recently, chevrons "in the conduction regime" have been reported "in the homeotropic geometry" [6-7].

Now we need to remind a free rotational mode of the director in the homeotropic geometry [6-10]. It can be induced from the *Fréedericksz* transition (FT; $V_F \sim 4$ V in the present study) before EC occurs, and plays an important role in the homeotropic EC. If the rotation of rolls due to the rotational mode is periodic in some cases (see below), it is possible to generate the chevron patterns in the conduction regime. In the case of the irregular rotation of the rolls in the *xy*-plane, however, the so-called soft-mode turbulence always appears in the homeotropic geometry [10-12].

In this paper the chevrons observed in the homeotropic geometry are investigated by varying electric conductivity for nematics. We found two types of the chevrons in the conduction regime ($f < f_c$) as well as the conventional chevron in the dielectric regime ($f > f_c$) mentioned above. In

order to describe the chevron patterns more precisely than past classification [13] in which they were defined by the size of the wavelength [chevron-A: large λ_1 ($\leqq d$) ; chevron-B: much small λ_1 ($\ll d$)], the detailed classification will be given.

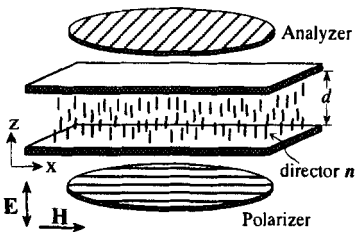

FIGURE 1 An electric field **E** and a magnetic field **H** are applied perpendicularly and parallel to the electrodes, respectively. Crossed polarizers are set, which can be rotated or removed readily.

EXPERIMENT

A slab of a nematic liquid crystal MBBA (*p*-methoxybenzilidene-*p*'-*n*-butylaniline) was sandwitched by two transparent electrodes which were treated with homeotropic alignment. In the present study three samples with different electric conductivity were prepared, which could be controlled by doping of TBAB (tetra-*n*-butyle-amonium bromide). See the details of the samples in Tab. 1. The temperature of the sample was stabilized at 30±0.1°C by an electric control system (Digital Controller DB500). The sample thickness was $d = 50$ μm and the lateral size of the samples was 1 × 1 cm^2. The experimental setup is shown in Fig. 1. The patterns were observed in the *xy*-plane by use of a CCD camera (SONY XC-75) mounted on a microscope.

RESULTS AND DISCUSSION

The threshold V_c for onset of patterns was determined in three samples, as shown in Fig. 2. The threshold $V_c(f)$ of the sample 1 with low conductivity shows a well-known frequency dependence (see, e.g., Refs. [1, 4]). The cut-off frequency f_c shifts to higher frequency with increasing con-

TABLE 1 Electric conductivities and dielectric constants of three samples at T = 30 °C

	sample 1	sample 2	sample 3
$\sigma_{//}$ [$\Omega^{-1}m^{-1}$]	7.49×10^{-9}	6.25×10^{-8}	9.08×10^{-7}
$\sigma_{\perp}$ [$\Omega^{-1}m^{-1}$]	6.38×10^{-9}	3.17×10^{-8}	7.37×10^{-7}
$\varepsilon_{//}$	3.84	3.78	4.33
$\varepsilon_{\perp}$	4.18	4.03	4.62

ductivity. f_c of the sample 2 and 3 with high conductivity could not be determined because of limit of applied voltage. In the dielectric regime ($f > f_c$), the conventional chevrons with a small wavelength of striated rolls ($\lambda_1 \ll d$) were observed as shown in Fig. 3(a). Since the dielectric chevron (DC) in the homeotropic system has no preferred direction unlike in the planar case, [1, 14] the periodic defect lines are arbitrarily selected [13]. Except such an aspect, the DC in principle has no difference between planar and homeotropic geometries.

Now let us consider chevrons in the conduction regime ($f < f_c$). Two types of chevrons were observed below and above a certain characteristic frequency f_w ($< f_c$) in the sample 2 and 3. In the range $f_w < f < f_c$ of the sample 3 ($f_w \sim 3150$ Hz) one typical chevron pattern (defect-free chevron; DFC) was observed as shown in Figs. 2 and 3(b). The DFC is characterized by the stripes with alternating zig and zag rolls. For $f < f_w$, on the other hand, the other type of chevrons (defect-mediated chevron; DMC) was found as shown in Figs. 2 and 3(c). The spatially-periodic defect lines between alternating zig and zag rolls distinguishes DMC from DFC.

First, in order to investigate spatial characteristics of DFC and DMC, the two wavelengths $\lambda_1(f)$ and $\lambda_2(f)$ were measured at a fixed control parameter $\varepsilon \equiv (V^2 - V_c^2) / V_c^2 = 0.10$. Figure 4 shows the dependence of λ_1 and λ_2 on frequency f. There are two characteristic frequencies $f_L \sim 1450$ Hz, called the *Lifshitz* frequency [8, 15], and $f_w \sim 3150$ Hz. The short wavelength λ_1 decreases continuously with increasing f, although there exist

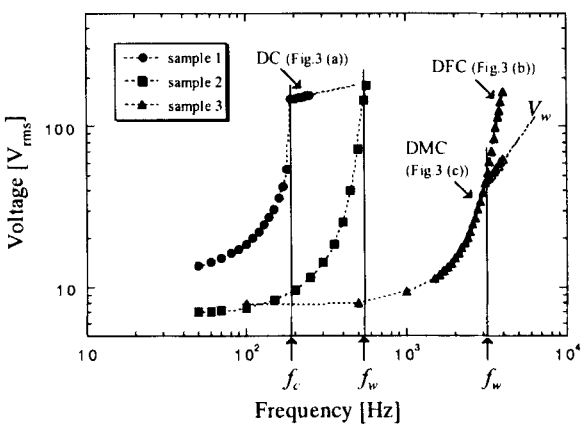

FIGURE 2 Thresholds of pattern formation on three samples. DC: dielectric chevron ($f > f_c$), DMC: defect-mediated chevron ($f < f_w$), DFC: defect-free chevron ($f_w < f < f_c$). Each chevron is showed in Fig. 3. See the text for details.

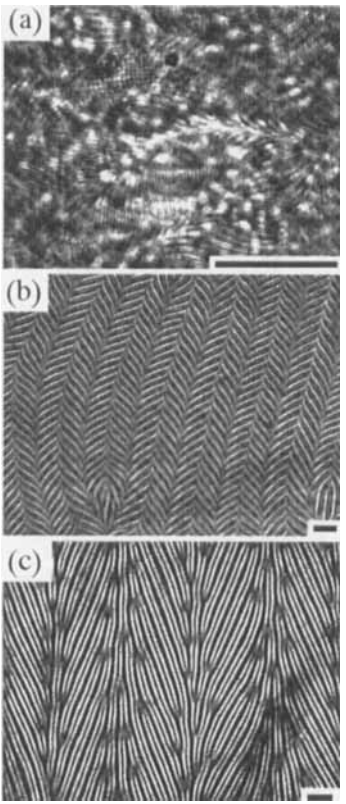

FIGURE 3 Three types of chevrons. (a) Dielecric chevron (DC), (b) defect-free chevron (DFC), (c) defect-mediated chevron. See also Fig. 2. Each scale bar is 100 μm.

the distinct characteristic frequencies (f_l and f_w) due to the different physical mechanisms [11, 10, 15]. But λ_1 weakly depends on f for $f < f_l$, while it strongly depends on f for $f > f_l$. The short wavelength λ_1 of the the striated rolls of chevrons is roughly of order d, the sample thickness ($d < \lambda_1 < 2d$). It is distinguishable from $\lambda_1 \ll d$ for DC in the dielectric regime. The long wavelength $\lambda_2(f)$ shows quite different frequency-dependence below and above f_w. For $f > f_w$ (DFC), λ_2 increases continuously with decreasing f and diverges at f_w. The dependence $\lambda_2(f)$ for DFC satisfies the following expression,

$$\lambda_2(f) = \xi_1 [(f - f_w)/f_w]^{-1/4} , \quad (2)$$

where $f_w = 3152$ Hz is determined from the fitting function, and a characteristic length $\xi_1 = 152$ μm ($\sim 3d$). For $f < f_w$ (DMC), on the other hand, λ_2 increases continuously with decreasing f and diverges at f^* with dependence

$$\lambda_2(f) = \xi_2 [(f - f^*)/f^*]^{-1/2} , \quad (3)$$

where $f^* = 1842$ Hz, and $\xi_2 = 408$ μm($\sim 4d$) . Here ξ_2 is a characteristic length which must be determined by the material parameters. Since $f^* > f_l$, no chevrons are found in the oblique-roll region ($f < f_l$), and chevronlike patterns are often found near f_w in the normal-roll region ($f_l < f < f_w$). Considering the different frequency-dependence and the characteristics of the patterns below and above f_w, the mechanism of DFC is clearly different from that of DMC.

Next, we have investigated the evolution process of both chevrons with increasing voltages, as shown in Figs. 5 and 6 (see Ref. [16] for the detail of the optical treatment). In the case of DFC ($f > f_w$) an instability is

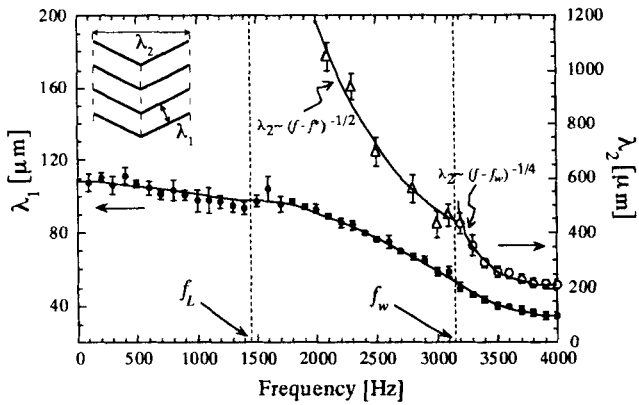

FIGURE 4 f-dependence of double periodicity (λ_1 and λ_2) of DMC ($f < f_w$) and DFC ($f > f_w$). Two wavelengths λ_1 and λ_2 were measured at a fixed $\varepsilon = 0.1$ and $H = 0$.

always induced before EC, which determines the long wavelengh λ_2 to form chevrons (DFC). We call this patterns in Fig. 5(a) the "prewavy" which shows a periodic director-modulation in the xy-plane. It should be distinguished from the conventional instability for EC with a periodic director-modulation in the xz-plane [11]. In Fig. 2, $V_w(f)$ corresponds to the threshold of the prewavies in sample 3. Consequently, we have found a sequent bifurcation; FT→ prewavy → DFC. For $f < f_w$, on the other hand, we have found a different bifurcation sequence into DMC with increasing ε. With the aid of weak magnetic field $H_x = 400$ G which stabilizes the $\boldsymbol{C}$-director (the projection of the director $\boldsymbol{n}$ onto the xy-plane) toward the x-axis, we have observed a sequent bifurcation with no background patterns like prewavies, as shown in Fig. 6 ; FT→ normal rolls (NR) → abnormal rolls (AR) → defect chaos → DMC. It is manifest that the mechanism of DMC is different from that of DFC [17]. The study of the prewavy instability to form DFC is now in progress.

SUMMARY

We have described the three types of our chevrons (DMC, DFC and DC) in terms of the characteristics of patterns and the dependence of electric conductivity and evolution process. The DMC is characterized by spatially-periodic defect lines between alternating zig and zag rolls, while the DFC is characterized by alternating zig and zag rolls without defects. More-

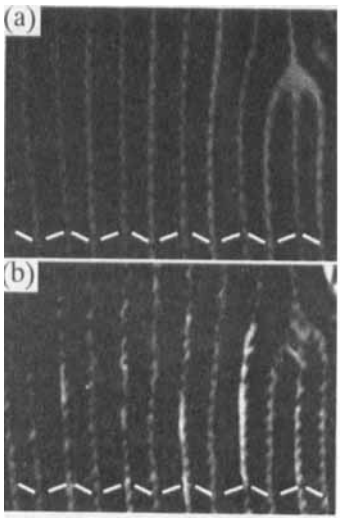

FIGURE 5 Pattern evolution into DFC with increasing ε ($f = 3500$ Hz). (a) $\varepsilon = -0.1$, (b) $\varepsilon = 0.05$. These patterns were obtained in crossed polarizers. The lods represent the ***C***-directors and thier directions.

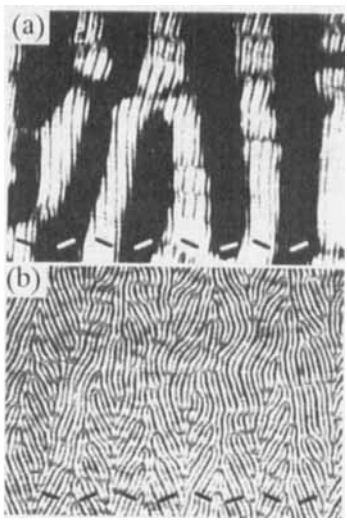

FIGURE 6 Pattern evolution into DFC with increasing ε ($f = 2000$ Hz). (a) Defect chaos in crossed polarizers at $\varepsilon = 0.1$, (b) DMC in no polarizer at $\varepsilon = 0.2$.

over, they show quite different frequency dependence. These DMC and DFC could be distinguished from the conventional DC by the size of short wavelength λ_l. Futhermore, generic bifurcation sequences for the two types of chevrons as well as the conventional DC are found with increasing voltage, that is, FT → NR → AR → defect chaos → DMC for $f < f_w$, FT → prewavy → DFC for $f > f_w$, and FT→ DC for $f > f_c$ (FT→ prewavy → DC may be found in the case of high conductivity samples, but we could not observed because of limit of applied voltages). From our results we have clearly classified our chevrons in Tab. 2.

The double periodic-structures, chevorns, are formed by a superposition of more than two instabilities. And one of them must be related the rotation of the ***C***-director which forms the obliqueness of the rolls of chevrons. We have concluded that the prewavy instability plays a role on the the rotation of the ***C***-director for DFC, while the abnormal roll instability and generating defects play the role for DMC. Moreover, the axes of zigzag rolls of each chevron are always roughly normal to the ***C***-director.

TABLE 2 New classification of chevrons. Though DC in this paper was directly evolved from *Fréedericksz* transition, it must be also found via prewavy in high conductivity samples.

	DMC	DFC	DC
frequency	$f<f_w$	$f_w<f<f_c$	$f>f_c$
λ_1	$\leqq 2d$	$< d$	$\ll d$
λ_2	$\sim (f-f^*)^{-1/2}$	$\sim (f-f_w)^{-1/4}$	?
defects	existence	no existence	existence
evolution	FT → NR → AR → Defect chaos → DMC	FT → Prewavy → DFC	FT → (Prewavy) → DC

• DMC: defect-mediated chevron, DFC: defect-free chevron, DC: dielectric chevron, FT: *Fréedericksz* transition, NR: normal rolls, AR: abnormal rolls

Acknowledgements

This work is partially supported by the Grant-in Aid for Scientific Research from the Ministry of Education, Sports and Science in Japan (Nos. 08454107 and 1044017).

References

[1] L.M. Blinov, *Electro-optical and magneto-optical properties of liquid crystals* (The Universities Press (Belfast) Ltd., Northern Ireland, 1983).

[2] P.G. de Gennes and J. Prost, *The Physics of Liquid Crystals* (Oxford University Press, New York, 1993) 2nd ed.

[3] M.C. Cross and P.C. Hohenberg, Rev. Mod. Phys., **60**, 851 (1993).

[4] L. Kramer and A. Pesch, Ann. Rev. Fluid Mech., **27**, 515 (1995).

[5] S. Kai and W. Zimmermann, Prog. Theor. Phys. Suppl. No. **99**, 458 (1989).

[6] J. -H. Huh, Y. Hidaka and S. Kai, Phys. Rev. E, **61**, 2769 (2000), and therein references. .

[7] P. Toth, A. Buka, J. Peinke and L Kramer, Phys. Rev. E, **58**, 1983 (1998).

[8] A. Hertrich, W. Decker, W. Pesch and L. Kramer, J. Phys. II **2**, 1915 (1992).

[9] H. Richter, N. Klopper, A. Hertrich and A. Buka, Europhys. Lett., **30**, 37 (1995).

[10] A.G. Rossberg, A. Hertrich, L. Kramer and W. Pesch, Phys. Rev. Lett., **76**, 4729 (1996).

[11] S. Kai, K. Hayashi and Y. Hidaka, J. Phys. Chem., **100**, 19007 (1996).

[12] Y. Hidaka, J. -H. Huh, K. Hayashi, M.I. Tribelsky and S. Kai, Phys. Rev. E, **56**, R 6256 (1997); J. Phys. Soc. Jpn., **66**, 3329 (1997).

[13] K. Hirakawa and S. Kai, Mol. Cryst. Liq. Cryst., **40**, 261 (1977).

[14] M. Scheuring, L. Kramer and J. Peinke, Phys. Rev. E, **58**, 2018 (1998).

[15] J.-H. Huh, Y. Hidaka and S. Kai, J. Phys. Soc. Jpn., **68**, 1567 (1999).

[16] J.-H. Huh, Y. Hidaka and S. Kai, Phys. Rev. E, **58**, 7355 (1998).

[17] A.G. Rossberg and L. Kramer, Physica D, **115**, 19 (1998).